Isolation and Characterization of Polymeric and Particulate Components of Acrylonitrile–Butadiene–Styrene (ABS) Plastics by Thermal Field-Flow Fractionation

PAUL M. SHIUNDU,[1,*] EDWARD E. REMSEN,[2] and J. CALVIN GIDDINGS[1,†]

[1]Field-Flow Fractionation Research Center, Department of Chemistry, University of Utah, Salt Lake City, Utah 84112; [2]Analytical Sciences Center, Monsanto Corporate Research, Monsanto Company, 800 North Lindbergh Blvd., St. Louis, Missouri 63167

SYNOPSIS

Thermal field-flow fractionation (ThFFF) is shown here to be capable of isolating the polymeric and rubber particulate components of acrylonitrile–butadiene–styrene (ABS) plastic in a simple analytical procedure. To facilitate the separation, the ionic strength of the two carrier liquids used here (THF and DMF) was brought up to 0.10 mM to increase the retention of the rubber particles. At a field strength (temperature drop) ΔT of 50 K, the two components were well separated, although the polymer component was not completely resolved from the void peak due to its low molecular weight. To facilitate a more rapid separation of the components, both field programming and high flow-rate conditions were examined in some detail. Both the particle-size distribution (PSD) of the rubber particles and the molecular weight distribution (MWD) of the polymer components were obtained using ThFFF. Measured MWD and PSD agreed favorably with PSD determined by dynamic light scattering and MWD obtained by size-exclusion chromatography. © 1996 John Wiley & Sons, Inc.

INTRODUCTION

ABS Analysis

Acrylonitrile–butadiene–styrene (ABS) polymers constitute a well-known class of toughened plastics used in applications requiring stiffness and fracture resistance. These materials are commercially important because their performance properties can be tailored to meet specific application needs by varying the particle-size distribution (PSD) of the rubber (butadiene) fraction and/or the molecular weight distribution (MWD) of the styrene–acrylonitrile (SAN) polymer matrix.[1]

The intrinsic versatility of ABS plastics has led to commercial development efforts directed toward customizing the material to suit specific applications. This customization requires reliable and convenient analytical methods for the determination of PSD and MWD. A variety of analytical techniques have been used in pursuit of this goal. Electron microscopy (scanning[2] and transmission[3,4]), light scattering,[5] and electrozone (coulter) analysis[6] have been employed for PSD analysis. Gel permeation chromatography[7] (GPC) has been used for characterizing the MWD of the soluble SAN matrix. Although these techniques have been widely employed, they are limited in an analytical sense because the PSD and MWD of the polymer cannot be determined in a single analysis using only one method. In addition, some of the above-mentioned methods are complicated multistep procedures that require separation of the gel (rubber) and soluble polymer (SAN matrix) fractions of the ABS prior to analysis. Rapid analysis (e.g., less than 1 h) of PSD and MWD under these constraints is not possible.

* Present address: Department of Chemistry, University of Nairobi, P.O. Box 30197, Nairobi, Kenya.
† To whom correspondence should be addressed.

Journal of Applied Polymer Science, Vol. 60, 1695–1707 (1996)
 CCC 0021-8995/96/101695-13

In an attempt to address these problems, a relatively new polymer and particle separation and characterization technique known as thermal field-flow fractionation (ThFFF) is introduced in this study for potential use in ABS analysis. A brief description of the principles of operation of field-flow fractionation is provided below.

Field-Flow Fractionation

Field-flow fractionation (FFF) is a family of separation techniques applicable to the separation of macromolecules and particles. FFF spans a wide mass/size range in which sample components are subjected to the combined effects of (1) an external field (or gradient) applied perpendicular to the axis of a narrow ribbonlike channel structure and (2) the axial flow of a carrier liquid flowing through the open channel.[8] The velocity profile of the carrier in the channel is approximately parabolic, with the higher flow regimes located in the channel center, and the slowest, near the walls. Separation of sample components occurs when different sample populations are selectively driven into different flow laminae by the external field. Each field (or gradient) yields a unique FFF technique. The most commonly used FFF "fields" are thermal gradients, cross-flow driving forces, electrical fields, and sedimentation fields, which yield the techniques ThFFF, flow FFF, electrical FFF, and sedimentation FFF, respectively.

In ThFFF, the external "field" is a temperature gradient applied across a channel enclosed between two parallel, highly polished metal bars. As a result of thermal diffusion, macromolecular and particulate components in a carrier liquid are forced differentially toward one wall (the accumulation wall) of the channel, leading to separation. The theoretical and experimental aspects of the ensuing separation process were discussed elsewhere.[8-12]

ThFFF, which in the past was used exclusively for the analysis and characterization of synthetic polymers,[13-15] was found recently to be applicable to the retention and fractionation of particulate matter, separating a variety of particle types both according to size (in both submicron and micron-size ranges) and chemical composition. The particles may be suspended either in aqueous or nonaqueous carrier liquids.[16-18] In addition, the separation of microgels and the soluble fractions of polymers[19,20] was successfully achieved. Because the ability to retain and fractionate both polymeric and particulate materials suggests that ThFFF is applicable to the analysis of complex composite materials, ThFFF was used here to try to isolate and characterize polymer and rubber particle components of ABS.

Theory of ThFFF

For highly retained species in ThFFF, retention is described approximately by[21]

$$\frac{t^0}{t_r} = \frac{6D}{D_T w(dT/dx)} \approx \frac{6D}{D_T \Delta T} \tag{1}$$

where t^0 is the channel void time (elution time for nonretained species); t_r, the experimental retention time; D, the concentration diffusion coefficient of the retained component; D_T, its thermal diffusion coefficient; dT/dx, the temperature gradient; ΔT, the temperature drop between the hot and cold walls; and w, the channel thickness (usually 50–200 μm).

For most polymeric materials, the diffusion coefficient D can be expressed as[22,23]

$$D = \frac{A}{M^b} \tag{2}$$

where A and b are constants for a given polymer/solvent system (generally, $0.5 < b < 0.7$) and M is the molecular weight of the polymer. Combining eqs. (1) and (2), we obtain an expression that relates t_r to M:

$$t_r = \frac{t^0 D_T \Delta T M^b}{6A} \tag{3}$$

If A, b, and D_T are known, M can be predicted from the experimentally measured retention time t_r.

In the case of particles, the ordinary diffusion coefficient D is related to the hydrodynamic particle diameter d by the Stokes–Einstein's expression

$$D = \frac{kT}{3\pi\eta d} \tag{4}$$

where k is Boltzmann's constant; T, the absolute temperature in the region occupied by the particles; and η, the viscosity of the suspending medium. By combining eqs. (1) and (4), we obtain

$$t_r = \frac{t^0 \pi \eta d D_T \Delta T}{2kT} \tag{5}$$

which relates the measured t_r to d.

To determine d at a given t_r, and thus obtain the PSD of a particulate material, D_T must be known. However, due to the lack of a sound theoretical basis for D_T, this term has to be obtained empirically for both polymers (to get M and MWD) and particles. (While D_T has been determined to be dependent on the composition of both polymer/solvent and particle/solvent systems, it is independent of M and the branching configuration for polymers but dependent on d for particles.[16–18]) This uncertainty in the value of D_T means that a calibration plot obtained with appropriate standards (or by other means) for both polymers and particles is needed for complete MWD and PSD analysis.

Experimental Goals

In this article, we describe initial steps in the development of ThFFF for the accurate and rapid characterization of the MWD and PSD of ABS plastics. To facilitate the development of effective ABS analysis by ThFFF, the effects of several parameters on the retention behavior of the particulate and soluble polymer fractions were investigated. The experiments performed were designed to evaluate the effects of salt concentration, field strength ΔT, flow rate, power programming, and solvent type. The primary solvent (or dispersion medium) was tetrahydrofuran (THF) but dimethylformamide (DMF) was used as an alternate solvent. A detailed description of the relevant experiments is provided later.

The influence of the ionic strength of the carrier liquid on the retention of the sample components was found to be particularly important. Previous studies on the retention of various particles (latex, silica, and metallic) suspended in aqueous or nonaqueous carrier liquids by ThFFF have demonstrated the importance of adding salt to the carrier liquid to achieve particle retention. The weakness in (or apparent lack of) particle retention in salt-free carrier liquids has been attributed to particle-wall electrostatic interactions (of a repulsive nature) within the ThFFF channel.[18] These interactive forces are thought to repel the charged particles away from the accumulation wall into the faster streamlines of the parabolic flow profile, thereby causing the particles to elute too early for effective separation. Modification of the ionic strength controls the electrical double layer thickness (on both wall and particle surfaces) and thereby minimizes the effects of these repulsive forces on particle retention. Polymer components, by contrast, are not influenced by ionic strength, presumably because they are uncharged. Thus, ionic strength becomes a tool to manipulate the relative retention of particles and polymers such that their mutual separation can be achieved.

EXPERIMENTAL

Sample Preparation

The two acrylonitrile–butadiene–styrene (ABS) samples used in this study, designated as ABS1 and ABS2, were supplied by Monsanto Co. (St. Louis, MO). The two samples differed mainly in their particle-size ranges, with ABS2 covering a wider particle-size range than does ABS1. Size-exclusion chromatography (SEC) employing polystyrene calibration was used to characterize the molecular weight distribution of the soluble polymer components of ABS1 and ABS2. Molecular weight averages for these components, average copolymer composition, and rubber particle (or gel) content of ABS1 and ABS2 are summarized in Table I.

Dispersions of ABS were prepared by the addition of 50 mg samples into 20 mL vials of UV-grade THF (Burdick & Jackson Labs). The vials were sonicated in a Cole Parmer Model 8845-4 ultrasonic cleaner for 24 h to completely disperse large THF-swollen gel particles. The soluble and particulate fractions of ABS1 (i.e., ABS1P and ABS1R, respectively) and ABS2 (ABS2P and ABS2R, respectively) were isolated by ultracentrifugation of the dispersions in THF. A Beckman Instrument Model L5-65 ultracentrifuge equipped with a Model TI-80 rotor operated at 26,000 rpm (62,000 g) and maintained at a temperature of 5°C was used for this purpose. Following ultracentrifugation for 3 h, the soluble fraction was decanted, the gel was resuspended in THF, and the ultracentrifugation was repeated. The collection of the soluble fraction and reultracentrifugation of the gel was repeated two additional times.

Table I Characteristics of ABS Plastic Samples

Plastic	Particle Content (Wt %)	Polymer Characteristics		
		Wt % Acrylonitrile	M_w [a]	M_n [a]
ABS1	78	30	64,300	28,100
ABS2	63	28	69,200	27,500

[a] Determined by SEC as described in Experimental section.

The combined THF-soluble fractions were evaporated to a film under a nitrogen stream and then dried overnight under vacuum. The gel was dried in the same way.

Apparatus

The ThFFF system used in this study is similar to that described previously.[17] The open FFF channel, which is layered between two chrome-plated copper blocks, was cut from a thin Mylar spacer so as to have a rectangular shape with tapered ends. The channel thickness is 76 μm, the tip-to-tip length is 44.6 cm, and the breadth is 2.0 cm. The flow rate of the carrier liquid was held at 0.185 mL/min (unless stated otherwise) and was delivered by a Model M-6000A pump from Waters Associates (Milford, MA). An injection valve with a sample loop (20 μL in volume) was used to inject samples into the channel for analysis. Components eluting from the ThFFF channel were monitored by either a 254 nm Model UV-106A1 detector from Cole Scientific (Calasaba, CA) or a UV-vis Spectroflow 757 absorbance detector from Applied Biosystems, Inc. (Ramsey, NJ). The latter was used with DMF, which has a UV cutoff at 268 nm.

The temperatures of the hot and cold walls were measured by thermocouples inserted into small wells drilled into the copper blocks. Resistance heaters (6000 W total) were used to power the hot block while the cold block was cooled by running tap water. The temperature of the cold wall T_c was maintained at 24 $\pm$ 1°C when the ΔT used was 60 K or less (otherwise, T_c was 29 $\pm$ 1°C).

Dynamic light scattering (DLS) was used to determine the particle-size distribution of the isolated rubber particles in ABS1 (ABS1R). The experimental apparatus consisted of a 128-channel Model BI2030AT digital correlator (Brookhaven Instruments Co.) interfaced to a homebuilt goniometer and fiber optic light collection system. Scattered light was collected at an angle of 90° and all measurements were performed at room temperature. The rubber particles were dispersed in THF (Burdick & Jackson) which was prefiltered through a 0.2 micron filter (Gelman Scientific).

Measured and calculated base lines of the autocorrelation function of scattered light intensity fluctuations agreed to within 0.1%. Analysis of the autocorrelation functions was accomplished with the DLS software program ISDA (Brookhaven Instrument Co.) which employed single-exponential fitting, cumulant analysis, and nonnegatively constrained least-squares particle-size distribution routines. The reported particle diameters are expected to be accurate to within $\pm$5% of the true values based on measurements of polystyrene latex standards (Duke Scientific Co.) dispersed in water.

Chemicals

Spectrograde THF from EM Industries (Cherry Hill, NJ) and DMF from Mallinckrodt Speciality Chemicals Co. (Paris, KY) were used as carrier liquids. The ionic strength of the carrier liquids was modified using tetrabutylammonium perchlorate (TBAP) from Fluka Chemical Corp. (Ronkonkoma, NY). Samples were provided by Mr. T. Weisse of Monsanto Co.

RESULTS AND DISCUSSION

Effect of Ionic Strength

Because various particles suspended in either aqueous or nonaqueous carrier liquids have shown little or no retention in salt-free carrier suspensions,[18] experiments were conducted to investigate the effect of different concentrations of TBAP on the retention of the ABS sample components, particularly, the polybutadiene particles. THF was used as the carrier liquid in this part of the study. Figure 1(a) and (b) show the effect of TBAP concentration on the retention of the rubber particulate components of ABS1 and ABS2 (i.e., ABS1R and ABS2R), respectively. The field strength ΔT was 50 K and the flow rate was 0.185 mL/min. Both figures show significant increases in retention time with concentration of TBAP. Figure 1(a) shows that in the absence of any salt the retention of one of the particulate components, ABS1R, is quite small. This is consistent with results for a variety of particles as noted above.[18]

Figure 2, by contrast, shows the independence of the retention time of the soluble polymer component of ABS1 (i.e., ABS1P) on TBAP concentration under the same conditions as reported for Figure 1. Similar observations were made for ABS2P. (It is not known if the retention of other polymers is also independent of the electrolyte.)

Because of the similarly weak retention of the particulate and the soluble polymer components of ABS in the absence of an electrolyte, we cannot expect to separate the two from their mixture in a salt-free medium. Figure 3 illustrates the problem,

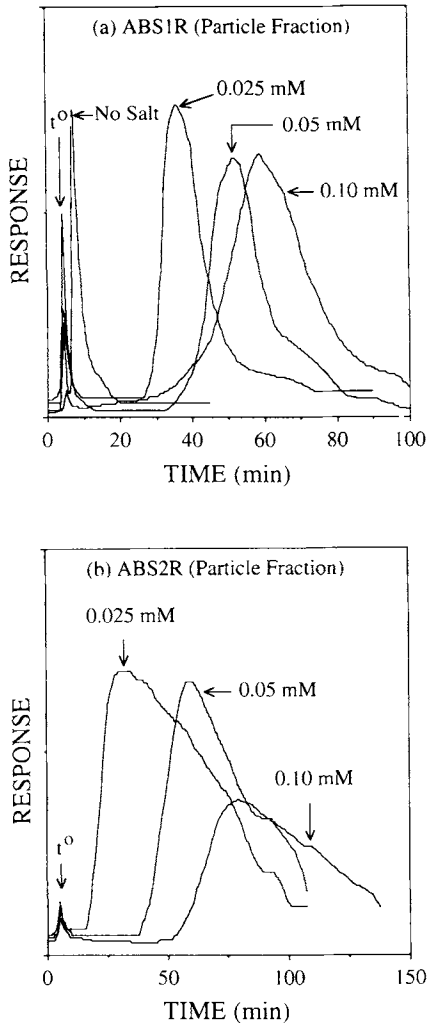

Figure 1 Effect of concentration of TBAP on the retention of rubber particulate fractions (a) ABS1R and (b) ABS2R in THF. Experimental conditions: ΔT = 50 K; flow rate = 0.185 mL/min.

showing the coelution of ABS1R (in salt-free THF) and ABS1P (run in 0.025 m*M* TBAP, recognizing that polymer retention is independent of electrolyte concentration) eluted against ΔT = 50 K and a flow rate of 0.185 mL/min. However, ABS1R is well separated from ABS1P in THF with a 0.025 m*M* concentration of TBAP. These results indicate that to effectively separate the particulate from the soluble polymer components an appropriate salt concentration must be employed.

The influence of salt concentration is further demonstrated by our observation of longer retention times for the rubber particles in THF at ΔT = 30 K and [TBAP] = 0.05 m*M* than with a salt-free THF carrier operated at ΔT = 120 K. However, optimum salt concentration and ΔT conditions require still further study.

Effect of ΔT

According to eqs. (3) and (5), the retention time t_r of a species in ThFFF should increase in proportion to ΔT. An increase in ΔT will not only enhance particle retention and thus provide a more complete separation of polymeric from particulate components, it will also increase the retention of the soluble polymers and improve their characterization. However, increases in ΔT, by prolonging retention (unless offset by a higher flow rate), can increase the experimental run time beyond desirable levels. Therefore, the effect of ΔT on both the retention time and resolution of the particle/polymer components was examined by carrying out experiments at different ΔT values. The criteria for preferred conditions were sped along with adequate resolution between the components.

Figure 4 shows superimposed elution profiles of the polymeric component ABS1P obtained in THF at three different ΔT conditions of 60, 90, and 120 K. It is apparent from this figure that the polymer fraction cannot be completely separated from the void peak (eluting at t^0), even at a ΔT as high as 120 K. This is attributed to the presence of low molecular weight polymer components. Similar results were

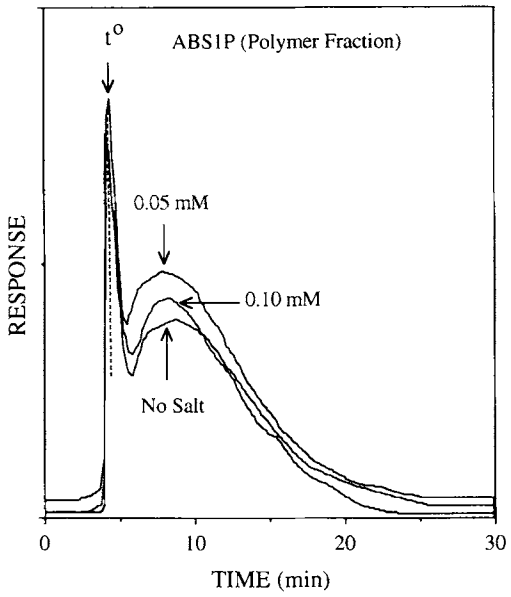

Figure 2 Effect of concentration of TBAP on the retention of soluble polymer fraction ABS1P in THF. Experimental conditions same as in Figure 1.

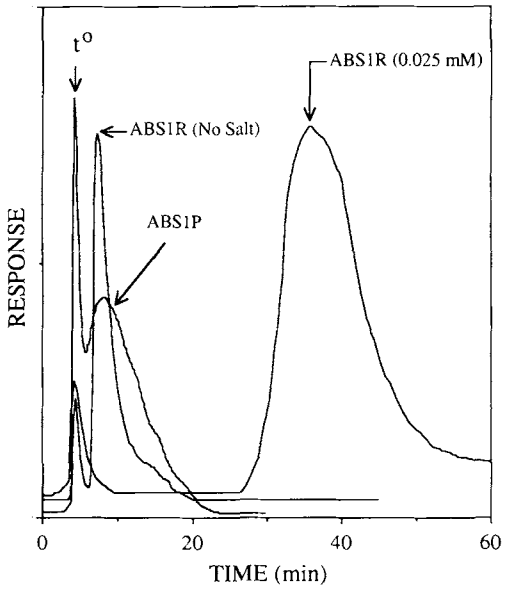

Figure 3 Fractograms of ABS1P (virtually identical with and without electrolyte) and ABS1R in both pure THF or electrolyte-containing THF. Experimental conditions: ΔT = 50 K; flow rate = 0.185 mL/min; [TBAP] = 0.25 m*M*.

obtained for ABS2P and are omitted for reasons of brevity.

Figure 5(a) and (b) show the effect of ΔT on the retention of the particulate components, ABS1R and ABS2R, in THF. The concentration of TBAP em-

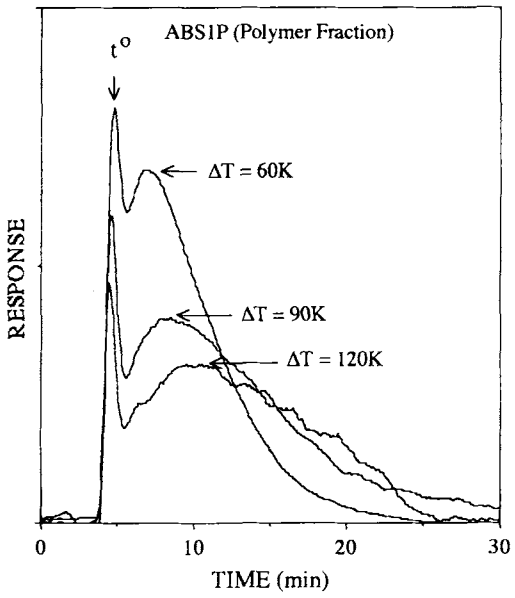

Figure 4 Effect of ΔT on the retention of ABS1P in THF. Experimental conditions: flow rate = 0.185 mL/min; [TBAP] = 0.10 m*M*.

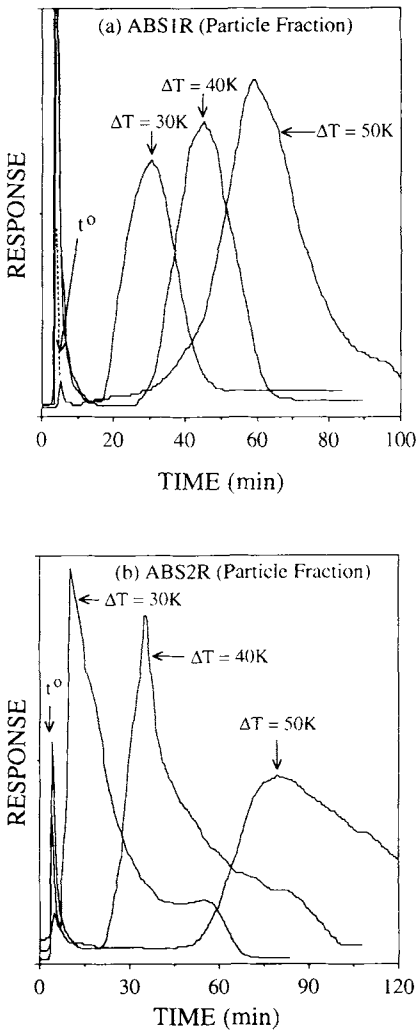

Figure 5 Effect of ΔT on the retention of (a) ABS1R and (b) ABS2R in THF. Experimental conditions: flow rate = 0.185 mL/min, [TBAP] = 0.10 m*M*.

ployed was 0.10 m*M*. As expected from theory, the retention times increased in rough proportion to ΔT. Under these ionic strength conditions, adequate retention for separation from the polymer (eluting near t^0) was achieved at relatively low ΔT. A comparison of Figures 4 and 5(a) indicates that a ΔT of 50 K is sufficient for the complete separation of the polymeric and particulate components (i.e., ABS1P and ABS1R) in THF when [TBAP] = 0.10 m*M*, despite the poor retention of the ABS1P component. The same is true for ABS2 sample components.

Figure 6(a) shows superimposed elution profiles of ABS1P, ABS1R, and ABS1 obtained in THF at ΔT = 50 K with [TBAP] = 0.10 m*M*. Similar plots for ABS2 and its components are provided in Figure 6(b). These elution profiles (or fractograms) show

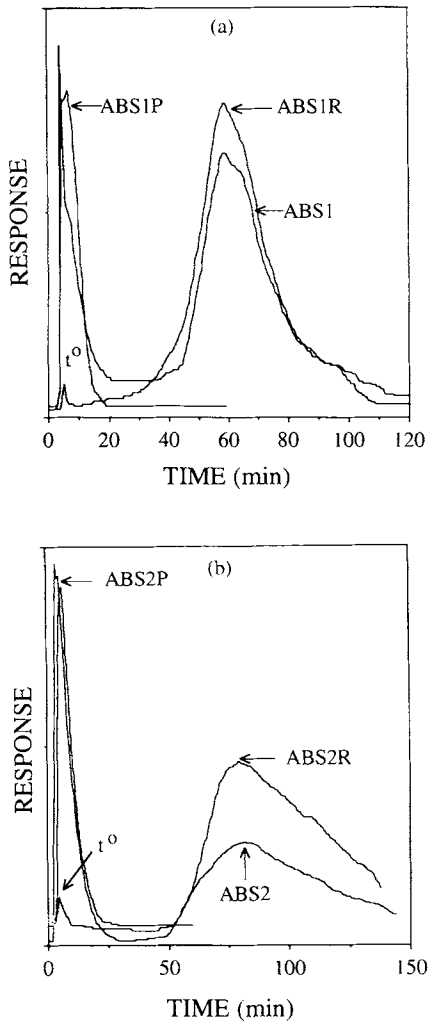

Figure 6 Superimposed fractograms of (a) components ABS1P, ABS1R, and the ABS plastic sample ABS1 and (b) components ABS2P, ABS2R, and the plastic sample ABS2. Experimental conditions: ΔT = 50 K; flow rate = 0.185 mL/min; [TBAP] = 0.10 m*M*.

that the chosen conditions are suitable for the complete separation of the polymeric and particulate components of the two ABS plastic samples examined here.

The total run times for the two sets of experiments reported in Figure 6 range between 100 and 150 min. Clearly, the above conditions of ΔT and flow rate yield long analysis times. To achieve a higher separation speed while maintaining an acceptable resolution between the sample components, a proper choice of the wide range of controllable parameters in FFF is needed. The parameters affecting separation speed and resolution include flow rate, channel thickness, ΔT, and carrier properties (e.g., ionic strength and solvent type). Procedures such as field programming can also be used to improve the speed of analysis for highly retained species. A complete optimization is beyond the scope of this article. However, in the next two sections, we provide results from both field programming and flow-rate studies that demonstrate an improved separation speed while maintaining a suitable level of resolution.

Field Programming

In the field programming operation, the field strength ΔT is systematically changed in the course of the run.[24] This serves not only to control and reduce the elution time of highly retained species but also to improve their detectability.

Figure 7 shows a plot of ΔT vs. time used in the parabolic field programming experiments conducted here. The initial field strength ΔT was held constant for 5 min at 50 K before it was allowed to systematically fall (according to a parabolic function) to a final ΔT of 5 K. Although ΔT was under computer control, it tended to have small deviations from the parabolic profile as shown in Figure 7. These deviations are inconsequential for practical analysis.

Figure 8(a) shows two fractograms of the particulate fraction ABS1R: one obtained under constant ΔT (isocratic) conditions (ΔT = 40 K) and the other

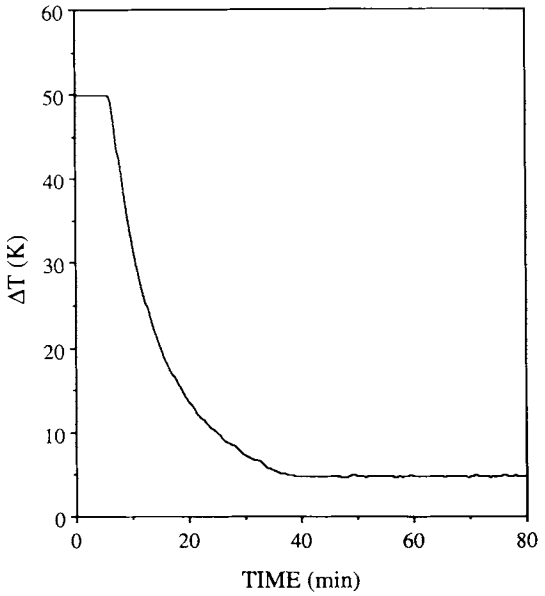

Figure 7 Profile of field strength ΔT as a function of time. The decay curve is roughly parabolic. Initial ΔT = 50 K; initial time lag = 5 min; final ΔT = 5 K.

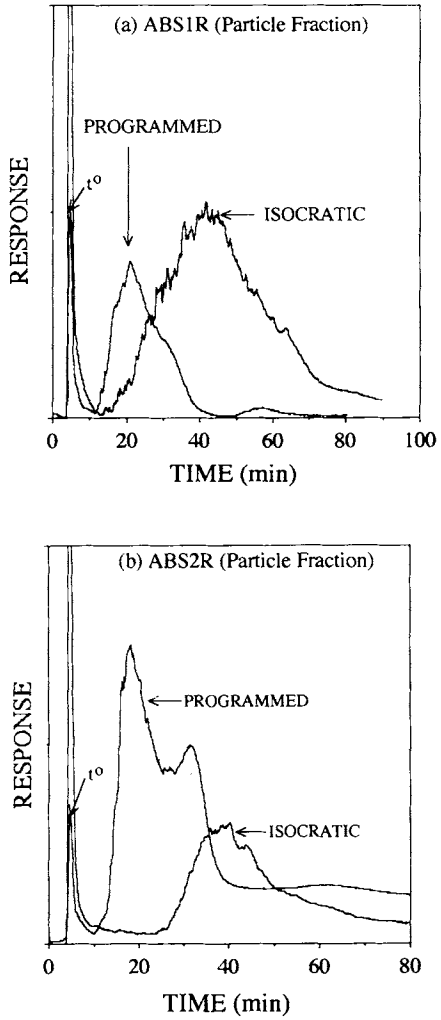

Figure 8 Fractograms of particle fractions (a) ABS1R and (b) ABS2R obtained in THF under both isocratic (ΔT = 40 K) conditions and parabolic programming of ΔT. Experimental parameters: flow rate = 0.185 mL/min; [TBAP] = 0.10 m*M;* programming conditions as shown in Figure 7.

under the programmed conditions described by Figure 7. The results show an improvement in speed for the power programmed run over the isocratic run (i.e., about 40 min compared to 100 min). Similar experiments were performed with ABS2R with comparable results as shown in Figure 8(b). In addition, Figure 8(b) shows evidence of a bimodal distribution of the ABS2R particulate component, although closer analysis (see later) shows that the second peak is only a shoulder on the PSD curve.

It should be noted that with a smaller initial ΔT, such as 40 K or below, the retention of the soluble polymer components is quite weak, making MWD analysis difficult. Thus, while power programming with a low initial ΔT would give a rapid isolation of the particles from the soluble polymers, a much higher initial ΔT of 90 K was used to increase the retention of the soluble polymer component. Furthermore, ΔT was held constant (at 90 K) for a relatively longer time (10 min) to allow time for polymer fractionation. The full ΔT profile is shown in Figure 9 superimposed on the ABS2 fractogram obtained by this programming modification. The run time is seen to be considerably reduced compared to that required under the isocratic conditions of ΔT = 50 K [see Fig. 6(b) for comparison]. The polymer component is also better retained due to the high initial ΔT. However, as suggested above, full optimization requires consideration of all variables affecting retention and resolution. One other important variable is the carrier liquid flow rate.

Effect of Carrier Flow Rate

To further improve separation speed, higher carrier flow rates were employed. Correspondingly larger ΔT values (70 vs. 50 K) were used to minimize excessive band broadening due to nonequilibrium effects.[25] Figure 10(a) and (b) show overlaid fractograms of the soluble polymer components and the corresponding ABS samples ABS1 and ABS2. The flow rate of the carrier liquid was 0.50 mL/min,

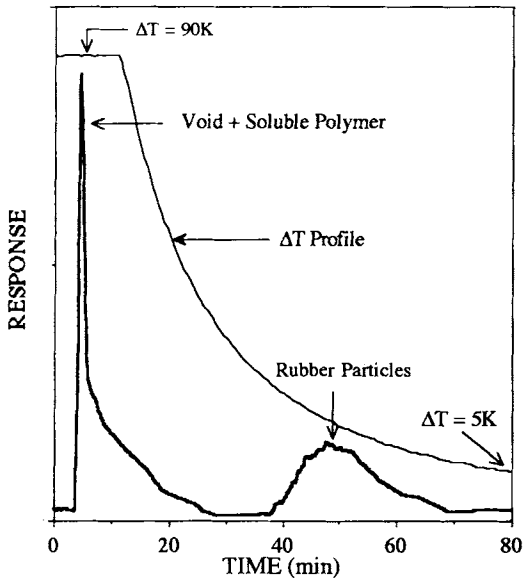

Figure 9 Fractogram of ABS sample ABS2 in THF using parabolic programming. Experimental conditions: flow rate = 0.185 mL/min; [TBAP] = 0.10 m*M;* initial ΔT = 90 K; initial time lag = 10 min; final ΔT = 5 K.

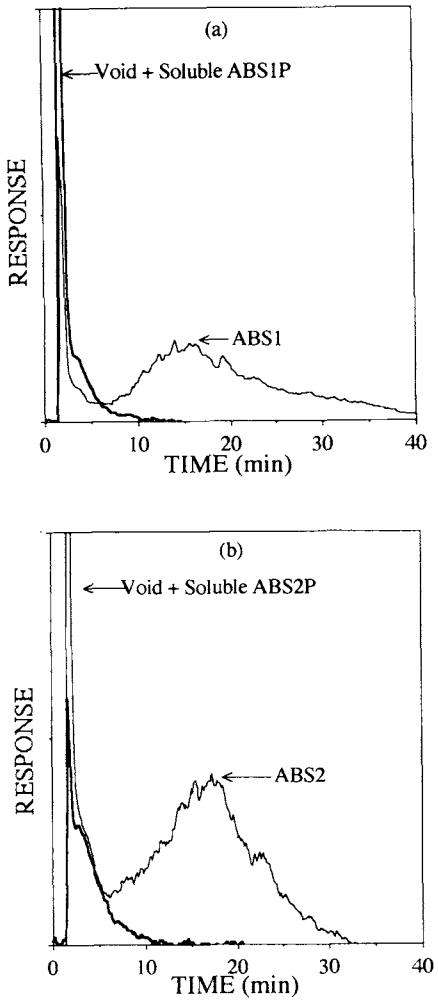

Figure 10 Fractograms of (a) polymer component ABS1P and the ABS plastic sample ABS1 and (b) polymer component ABS2P and the ABS plastic sample ABS2 obtained using THF. Experimental conditions: ΔT = 70 K; flow rate = 0.50 mL/min; [TBAP] = 0.10 m*M*.

about three times the value used in previous experiments. Both figures show a significant improvement in separation speed (under 40 min) compared to those found in Figure 6. The higher flow rate has led to a small degree of overlap between the polymeric and particulate components. However, the resolution is still quite good and is probably sufficient for most practical purposes.

Use of DMF as Carrier

DMF was investigated as an alternate carrier liquid because, unlike THF, it does not swell the rubber particles. The swelling of these particles by THF is likely to complicate the extraction of size-distribution information from the experimental fractograms. Therefore, a series of experiments paralleling those described above for THF were carried out using DMF. Electrolyte effects were found to be similar in the two solvents. The preferred concentration of TBAP in DMF, like THF, was 0.10 m*M*.

Figure 11(a) shows the retention profiles of standard polybutadiene (PB) latex particles (0.121, 0.232, and 0.410 μm in diameter) suspended in DMF. The flow rate was 0.29 mL/min and ΔT was 50 K. This figure demonstrates that ThFFF can effectively retain and separate PB particles in DMF. Furthermore, it suggests that by using narrow distributions of well-characterized particles a calibration relationship can be established and the PSD of an un-

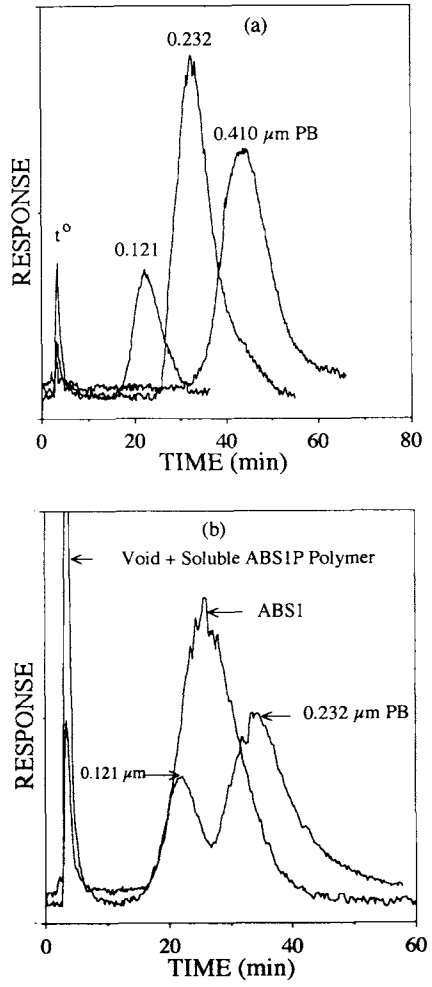

Figure 11 Elution profiles obtained using DMF. These show (a) separation of standard PB latex particles and (b) fractograms of ABS1 and of two standard PB latex particles. Experimental conditions: ΔT = 50 K; flow rate = 0.29 mL/min; [TBAP] = 0.10 m*M*.

known sample material of identical composition (such as the PB particles found in ABS) can be obtained. Figure 11(b), which shows superimposed fractograms of ABS1 and a mixture of 0.121 and 0.232 μm PB latex particles, indicates that the distribution of PB particles in the plastic ABS1 falls primarily between 0.1 and 0.25 μm. The PSD curve for ABS1 will be shown later.

Figure 12 further characterizes the retention properties of ABS components in DMF and suggests a significant departure from retention behavior in THF. Specifically, Figure 12 shows that the polymeric component ABS1P of the plastic ABS1 is not measurably retained in DMF with ΔT = 50 K. A similar lack of retention was found for ABS2P. The much stronger retention of these polymers in THF is illustrated in Figure 2, where the bulk of the polymer is seen to elute beyond the void peak (at time t^0) rather than coinciding with the void peak.

The particulate component of ABS is well retained, although somewhat less than for THF. Retention is sufficient to readily fractionate and characterize the particulate matter, even with ΔT as low as 50 K. This is illustrated by Figure 13, which shows fractograms for the two ABS plastics used as samples in this study. This figure confirms a much broader particle-size distribution for the plastic ABS2. It also suggests that the distribution for ABS2 has a second mode or a shoulder, a conclusion supported by Figure 8(b), which was obtained using THF.

The above results with DMF were all obtained with ΔT = 50 K and the flow rate set at 0.29 mL/min. The speed of execution of the experimental runs can be increased by using a higher flow rate; concurrent adjustments in ΔT can be made which will have a bearing on both speed and resolution. We carried out experiments on ABS1 and ABS2 plastics with the flow rate increased to 1.0 mL/min and with ΔT = 70 K. Under these conditions, the sample components are rather completely eluted in about 20 min, much faster than the elution shown in Figure 13. Further gains could likely be made with a more complete study of optimization.

The above study shows that DMF has advantages and disadvantages compared to THF as a solvent for the characterization of ABS by ThFFF. The disadvantage is that the polymeric component is not measurably retained and, thus, an MWD curve cannot be generated (although the total content of polymer could likely be obtained from void peak area). On the positive side, DMF yields a clean separation of the polymeric from the particulate components and, with proper calibration, will provide a PSD for the particles. The calibration should be more straightforward in interpretation because of the lack of swelling of the rubber particles in DMF (see below).

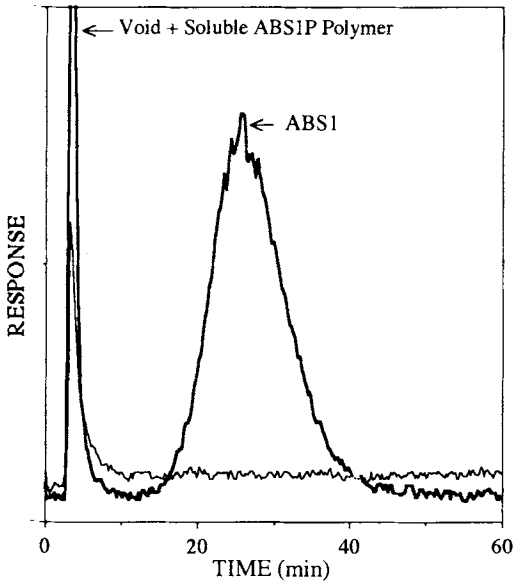

Figure 12 Fractograms of ABS1P and ABS1 in DMF. Experimental conditions: ΔT = 50 K; flow rate = 0.29 mL/min; [TBAP] = 0.10 m*M*.

Determination of PSD and MWD by ThFFF

Some of the studies necessary to make ThFFF a useful tool for ABS analysis are presented above. While additional studies are needed to optimize conditions, implement accurate calibration, and choose a single solvent suitable for both polymer MWD and rubber PSD determinations in a single rapid procedure, sufficient information is developed above to obtain MWD and PSD curves from separate runs. Even with separate runs, the ease of separation of the polymers from the rubber particles is advantageous because it eliminates the interference of one with the analysis of the other.

Figure 14(a) shows superimposed PSD curves for the rubber components of ABS1 and ABS2 (i.e., ABS1R and ABS2R, respectively) corresponding to the elution profiles shown in Figure 13. The retention times corresponding to the fractograms shown in Figure 13 were converted to particle sizes using calibration constants derived from the logarithmic plots of retention time vs. particle size based on data shown in Figure 11(a). In-house software was used to obtain the PSD curves. From the PSD plots,

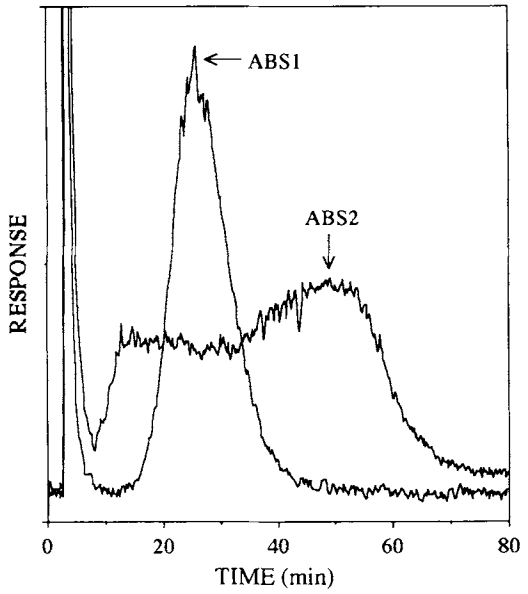

Figure 13 Fractograms of ABS1 and ABS2 in DMF. Experimental conditions same as in Figure 12.

ABS2R is found to have a particle-size distribution in the approximate range 0.03–0.80 μm, while ABS1R particles range between 0.05 and 0.35 μm. (Particle sizes above 0.55 μm are likely to be in error because of steric effects.)

Representative DLS PSD data for ABS1R were in good agreement with PSD determined by ThFFF. DLS yielded a range of particle diameters for ABS1R of 0.08–0.30 μm with a mean particle diameter of 0.16 μm.

A plot showing the MWD for the soluble ABS1P polymer component is provided in Figure 14(b). The MWD was obtained by applying our software to the fractogram shown in Figure 2. Standard polystyrene polymers covering the molecular weight range from 30,000 to 1000,000 were used to obtain the calibration constants necessary to generate the MWD curve. Polystyrene standards were deemed suitable because the retention times of SAN polymers of varying ratios of styrene to acrylonitrile showed independence of composition. MWD averages of ABS1P measured by ThFFF (M_w = 85,072 and M_n = 42,849) were larger than corresponding values obtained by size-exclusion chromatography employing polystyrene calibration (M_w = 64,300 and M_n = 28,100). The discrepancy between MWD averages is most likely due to the lack of separation of the lowest molecular weight polymer molecules in the void peak of the ThFFF fractogram (see Fig. 2), which would bias the MWD analysis toward higher molecular weight.

The calibration procedures utilized above may be subject to improvement. Since both particle and polymer retention depend on composition, standards must be appropriately chosen. The PB particles in ABS, e.g., may retain differently from PB standards because the former are grafted with SAN polymer. Better calibration plots may ultimately arise from

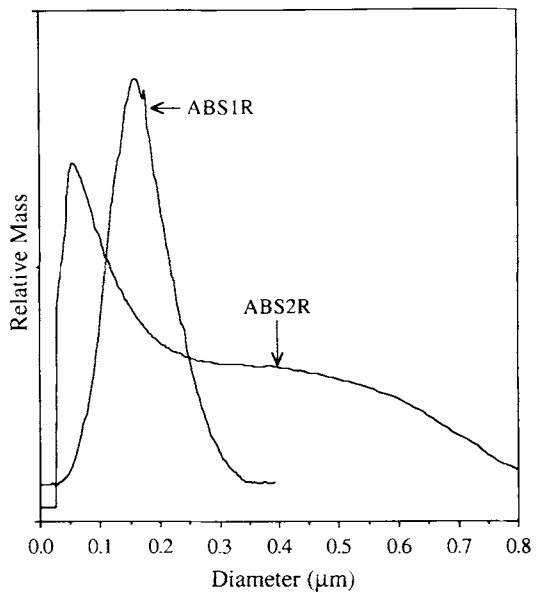

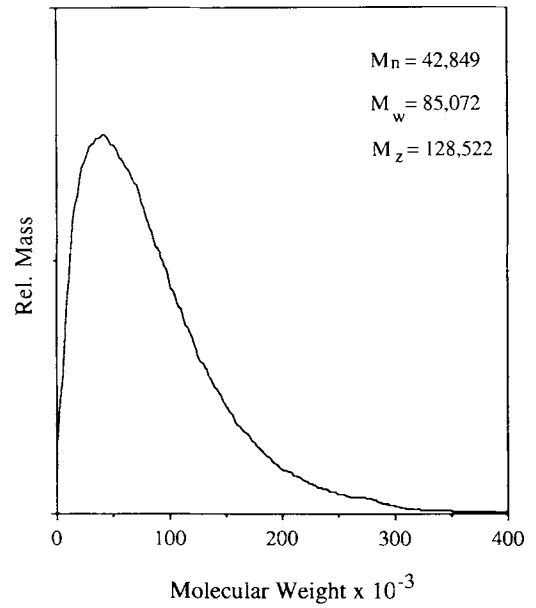

Figure 14 (a) Superimposed PSD plots for rubber components of ABS1 and ABS2 (i.e., ABS1R and ABS2R) corresponding to fractograms shown in Figure 13; (b) MWD plot for the soluble polymer component (ABS1P) corresponding to the fractogram shown in Figure 2.

the direct measurement of the particle size in collected fractions by electron microscopy. For copolymers, the dependence of retention on monomer ratio (although apparently weak for the SAN polymers studied here) needs to be considered for maximizing accuracy.

CONCLUSIONS

This study shows that thermal FFF is a technique having the capability of providing both the particle-size distribution of the rubber particles and the molecular weight distribution of the acrylonitrile–styrene polymers composing ABS plastic. The results obtained here suggest that ThFFF, with further study, could have significant advantages over present techniques for the characterization of ABS. Most promising is the possibility that the MWD of the polymers and the PSD of the particles could be obtained in a single run with a duration of less than 1 h. With further optimization studies, it is likely that the analysis time could be reduced to 10–20 min. Even if a single-run analysis proves impractical for some ABS materials, two rapid runs carried out concurrently or in sequence (using different experimental conditions) would independently provide the MWD and PSD. The additional work needed to implement these strategies involves both optimization studies and the acquisition of better calibration data for both the polymeric and particulate constituents.

In a broader context, ABS is but one example of a class of complex composite material having particles imbedded in a polymeric matrix to improve mechanical properties. The complete characterization of these materials requires MWD and PSD information on the polymeric and particulate constituents, respectively. In some cases, complete distributions may not be needed; one of the distributions along with the relative content of the two components may be sufficient. At almost any level of detail, the primary requirement is to gain a complete separation of the polymeric from the particulate material. Both this and previous studies[18] show that adjustments in the concentration of electrolytes in the applicable nonaqueous solvents provide an important tool for manipulating the retention of particulates and thereby maximizing the resolution of particulate matter from polymeric components. Since the composition of the solvent also has significant effects on retention (as shown here in comparing THF and DMF), solvent composition becomes another tool for the manipulation of retention and resolution. Clearly, a great deal of study is needed to fully exploit the potential of ThFFF (along with other FFF techniques) in the analysis of this broad category of complex composite materials.

NOMENCLATURE

ABS	acrylonitrile–butadiene–styrene plastic
d	particle diameter
dT/dx	temperature gradient in channel
D	ordinary diffusion coefficient
D_T	thermal diffusion coefficient
k	Boltzmann's constant
MWD	molecular weight distribution
PB	polybutadiene
PS	polystyrene
PSD	particle-size distribution
SAN	styrene-acrylonitrile polymer
t_r	retention time
t^0	channel void time
T	absolute temperature
T_c	cold wall temperature
w	channel thickness
ΔT	temperature drop across channel
η	viscosity

This work was supported in part by Grant No. CHE-9322472 from the National Science Foundation. The authors would also like to acknowledge Mr. T. Weisse of Monsanto Co. who supplied us with the ABS sample materials.

REFERENCES

1. C. B. Bucknall, in *Toughened Plastics,* Applied Sciences, London, 1977.
2. J. N. Sultan, R. C. Liable, and F. J. McGarry, *Appl. Polym. Symp.,* **16,** 143 (1973).
3. K. Kato, *J. Electron Micros.,* **14,** 220 (1965).
4. K. Kato, *Polym. Eng. Sci.,* **7,** 38 (1967).
5. K. Moritani, T. Inoue, M. Motegi, H. Kawai, and K. Kato, in *Colloidal and Morphological Behavior of Block and Graft Copolymers,* G. E. Molau, Ed., Plenum Press, New York, 1971, p. 33.
6. D. E. James, *Polym. Eng. Sci.,* **8,** 241 (1968).
7. D. L. and G. Riess, *J. Polym. Sci. (Chem.),* **11,** 3309 (1973).
8. J. C. Giddings, *Science,* **260,** 1456–1465 (1993).
9. J. C. Giddings, M. E. Hovingh, and G. H. Thompson, *J. Phys. Chem.,* **74,** 4271 (1970).
10. J. C. Giddings, K. D. Caldwell, and M. N. Myers, *Macromolecules,* **9,** 106 (1976).

11. L. K. Smith, M. N. Myers, and J. C. Giddings, *Anal. Chem.*, **49,** 1750 (1977).
12. J. J. Gunderson, K. D. Caldwell, and J. C. Giddings, *Sep. Sci. Technol.*, **19,** 667 (1984).
13. G. H. Thompson, M. N. Myers, and J. C. Giddings, *Sep. Sci.*, **2,** 797 (1967).
14. J. C. Giddings, M. Martin, and M. N. Myers, *J. Chromatogr.*, **158,** 419 (1978).
15. J. C. Giddings, M. N. Myers, and J. Janca, *J. Chromatogr.*, **186,** 37 (1979).
16. G. Liu and J. C. Giddings, *Anal. Chem.*, **63,** 296–299 (1991).
17. G. Liu and J. C. Giddings, *Chromatographia,* **34,** 483–492 (1992).
18. P. M. Shiundu, G. Liu, and J. C. Giddings, to appear.
19. X. Li and J. C. Giddings, *Thermal FFF of Microgels,* Poster presented at the Fourth International Symposium on Field-Flow Fractionation, Lund, Sweden, June 13–15, 1994.
20. S. Lee, in *Chromatography of Polymers: Characterization by SEC and FFF,* T. Provder, Ed., ACS Symposium Series 521, ACS, Washington, DC, 1993.
21. J. C. Giddings, K. A. Graff, K. D. Caldwell, and M. N. Myers, *Adv. Chem. Ser.*, **203,** 259 (1983).
22. P. J. Flory, *Principles of Polymer Chemistry,* Cornell University Press, Ithaca, NY, 1953, Chap. 14.
23. C. Tanford, *Physical Chemistry of Macromolecules,* Wiley, New York, 1961, p. 362.
24. J. C. Giddings, L. K. Smith, and M. N. Myers, *Anal. Chem.*, **48,** 1587–1592 (1976).
25. J. C. Giddings, *Anal. Chem.*, **58,** 735–740 (1986).

Received January 17, 1995
Accepted November 29, 1995